Dislocation pinning/depinning transition: Fixed-point analysis

Daniel G. Tekleab
Department of Physics and Astronomy, Clemson University, Clemson, South Carolina 29634

John W. Lawson
Department of Mathematical Sciences, Clemson University, Clemson, South Carolina 29634

Murray S. Daw*
Department of Physics and Astronomy, Clemson University, Clemson, South Carolina 29634
(Received 12 October 1999; revised manuscript received 6 January 2000)

We present a fixed-point analyis for the equations describing the motion of a dislocation in the presence of thermally activated cross-slip pinning events. Previously, a stochastic, finite-difference model was proposed [Chrzan and Daw, Phys. Rev. B **55**, 798 (1997)] in relation to the yield strength anomaly observed in $L1_2$ intermetallic compounds. (In such materials, the strength increases with increasing temperature.) In addition to numerical solutions, Chrzan and Daw also derived deterministic, mean-field equations to describe the dynamics. In this paper, we use a fixed-point stability analysis to solve analytically those mean-field equations. We compare the analytic solutions to the previously obtained numerical solutions. As with the (numerical) exact solutions, the mean-field solutions exhibit a pinning/depinning transition. Mean-field critical exponents and scaling relations are determined analytically.

I. INTRODUCTION

Recently, several models have been proposed[1–6] to describe dislocation motion under applied stress in the presence of cross-slip pinning. These models generally seek application to $L1_2$ intermetallic compounds, where the thermally activated cross-slip pinning results in increasing strength with increasing temperature. The equations are stochastic equations, either discrete or continuum. Numerical solutions have been obtained, which in all cases show the interesting characteristic of a pinning/depinning transition. At low stresses (or high temperatures) the dislocations become completely pinned by numerous cross-slip events. At high stresses (or low temperature), the dislocations remain indefinitely mobile (for an infinite sample). The transition between the two occurs abruptly. Evidence for critical scaling, and the relationship of this scaling to creep behavior was also explored.

The simple class of model proposed by Chrzan and Daw[5] (referred to here as CD), were discrete stochastic models with two governing parameters. In that work, the authors demonstrated numerically the existence of a pinning/depinning transition as well as dynamical scaling behavior, and they extracted the critical exponents of the transition numerically.

CD also developed a mean-field treatment of their model, which leads to a deterministic equation of motion. They solved these deterministic equations numerically and found the mean-field solutions also to exhibit a similar pinning/depinning transition and scaling.

The scaling behavior of the models has important physical consequences, as was pointed out especially by Chrzan, Mills, and Goods,[4] who showed how the scaling behavior was essential to understanding the various creep behaviors observed in the material. For that reason, it is interesting to study more the nature of the transition, and the form of the scaling relation.

The present paper will explore further the mean-field equation of motion proposed in CD. Simple approximations make the mean-field equations tractable. Using linear stability analysis near the fixed point, we study the pinning/depinning behavior analytically. Critical exponents and the scaling relations are determined as well.

The remainder of this paper is organized as follows. The next section reviews the class of models introduced by CD, including the mean-field approximation. Section III presents the analytic solutions to the mean-field equations and compares them to the numerical solutions of the exact equations. We end with a discussion.

II. THE CD MODEL OF DISLOCATION DYNAMICS WITH CROSS-SLIP PINNING

The models proposed and studied by CD attempt to capture four fundamental aspects of dislocation dynamics in the presence of external stress and cross-slip pinning. The first is the glide under external stress. The next is the cross-slip event, which happens with a probability q $(0<q<1)$. A cross-slipped node is considered immobilized. The third is the athermal stress-driven mobilization of a cross-slipped segment, which occurs when mobile segments of the dislocation advance beyond a locked segment and pull it loose. The fourth is the mobilization of a cross-slipped segment via a thermally activated process occurring with probability ε. It is expected generally that $\varepsilon \ll 1$. There are thus two governing parameters which control the dynamics of the model: $p(\equiv 1-q)$ and ε.

In the CD model, a dislocation is described by a discrete set of points which can move in the direction perpendicular to the average line direction. The slopes between the lines

TABLE I. Critical exponents for $B(3/2)$ and $B(2)$: analytic mean-field results compared to exact numerical results.

	$\varepsilon=0$ $(T=0)$	$\varepsilon>0$ $(T>0)$	MF analytic	Exact numerical
Velocity	$v(p)\sim(p-p_c)^{\nu}$	$v(p,\varepsilon)=\varepsilon^{\beta}f[(p-p_c)/\varepsilon^{\gamma}]$	$\beta=1/2$ $\gamma=1/2$ $\nu(=\beta/\gamma)=1$	$\beta\approx1/3$ $\gamma\approx1/3$ $\nu\approx1$
Characteristic time	$\tau(p)\sim\lvert p-p_c\rvert^{-\phi}$	$\tau(p,\varepsilon)=\varepsilon^{-\zeta}h[(p-p_c)/\varepsilon^{\gamma}]$	$\zeta=1/2$ $\phi(=\zeta/\gamma)=1$	$\zeta\approx2/3$ $\phi\approx2$

are also discrete. The number of allowed values for the slope determines the degrees of freedom of the dislocation and its behavior under an applied stress. The models can be classified according to the range of allowed slopes. The simplest model considered in the present work allows slopes of $-3/2$, $-1/2$, $1/2$, and $3/2$ and is referred to as $B(3/2)$. The next model in the sequence, $B(2)$, allows the slopes to be -2, -1, 0, 1, or 2. The allowed dislocations configurations are then described in complete analogy to a one-dimensional chain of spins, though the dynamics of course are not analogous.

The order parameter in these models is the average, steady-state areal velocity of the dislocation. The extensive numerical simulations presented in CD show that the B models at zero temperature ($\varepsilon\to0$) generally display a pinning/depinning transition as a function of p. The model show two states: a pinned and unpinned state (or an immobile and a mobile state) separated by a critical value p_c. In the mobile phase ($p>p_c$), as $p\to p_c$, the average velocity approaches zero as

$$v(p)\sim(p-p_c)^{\nu} \tag{1}$$

with ν determined numerically to be close to 1. Both below and above the critical point, the decay of fluctuations is characterized by a time scale which appears to diverge as

$$\tau(p)\sim(p-p_c)^{-\phi} \tag{2}$$

with ϕ being numerically close to 2.

The effect found by CD of introducing finite temperature is to remove the singular nature of the transition. However, it was found numerically that a vestige of the transition remains in the form of scaling behavior. For finite ε, the scaling behavior takes the forms

$$v(p,\varepsilon)=\varepsilon^{\beta}f[(p-p_c)/\varepsilon^{\gamma}], \tag{3}$$

$$\tau(p,\varepsilon)=\varepsilon^{-\zeta}h[(p-p_c)/\varepsilon^{\gamma}] \tag{4}$$

The critical exponents must satisfy $\nu=\beta/\gamma$ and $\phi=\zeta/\gamma$. The values of the exponents as determined from extensive numerical solutions of the exact stochastic equations of motion are displayed in Table I.

A mean-field treatment was shown by CD to provide a good approximation to the exact numerical simulations of the stochastic equations. The deterministic mean-field equations are based on pairs of slopes as the fundamental units. Consider a pair of neighboring slopes, with the left slope having a value l and the right slope r. The frequency of occurrence (i.e., population) of this pair of slopes is called ρ_{lr}. The equation of motion of ρ_{lr} is obtained by calculating the average transition rate from a pair of type (l,r) to (l',r'). The mean-field approximation neglects correlations between neighboring slope pairs. The equation of motion derived from this assumption is

$$\underline{\underline{\rho}}_{i+1}=G(\underline{\underline{\rho}}_i;p,\varepsilon). \tag{5}$$

The instantaneous dislocation velocity is a linear function of the population matrix (see CD).

The mean-field equations were solved numerically in CD. The mean-field solutions bear a good resemblance to the exact numerical results. In particular, the models display a pinning/depinning transition at a nonzero value of p_c. Similar fidelity is obtained for the mean-field treatment at finite ε.

As indicated in the introduction, an important question considered in CD and in related work is that of the scaling. In the next section, we obtain analytic solutions to the mean-field fixed-point equations and the relaxation time. In particular, we are able to analyze the scaling relations in detail.

III. ANALYTICAL MEAN-FIELD SOLUTION

The mean-field equation of motion [Eq. (5)] is a set of deterministic, nonlinear, coupled, iterative equations. The order parameters are the elements of the population matrix ρ_{lr}. For $B(M)$, there are $(2M+1)^2$ elements in the population matrix, but these elements are not independent. Three types of sum rules apply. First, the populations must add to 1. Second, the steady-state solutions display left-right symmetry, so that $\rho_{lr}=\rho_{\bar{r}\bar{l}}$ (where $\bar{l}=-l$, etc.). Third, the topology of the line requires $\Sigma_l(\rho_{lr}-\rho_{rl})=0$ for all r. For $B(3/2)$ this reduces to 7 the degrees of freedom, 12 for $B(2)$.

To aid in obtaining the analytic solution, we examine the numerical solutions to the mean-field equations near the transition. Not surprisingly, each element of the population matrix ρ_{lr} belongs to one of two classes: mobile or immobile configurations. The ''inner configurations'' (that is, those elements in the interior of the population matrix) are immobile configurations (stationary for $\varepsilon\to0$). The ''outer configurations'' (that is, those with at least one slope of the pair having its maximum allowed value) are mobile (finite average velocity). This observation suggests an approximation which initially might seem severe, but which is born out by examination of the numerical calculations of CD. We propose to reduce the degrees of freedom to 1, in order to obtain a

simple analytic (approximate) solution. From there, it will be possible in concept to loosen this restriction to obtain a less constrained solution.

The extreme approximation then is to take as the population matrix for $B(3/2)$:

$$\begin{pmatrix} y & y & y & y \\ y & x & x & y \\ y & x & x & y \\ y & y & y & y \end{pmatrix} \tag{6}$$

which satisfies the sum rules if $y=(1-4x)/12$, or for $B(2)$

$$\begin{pmatrix} y & y & y & y & y \\ y & x & x & x & y \\ y & x & x & x & y \\ y & x & x & x & y \\ y & y & y & y & y \end{pmatrix} \tag{7}$$

with $y=(1-9x)/16$.

Using the above form for the population matrix at one time step and inserting into the master equation [Eq. (5)] produces the population matrix at the next time step, which will differ slightly from the constrained form above. For this reason, the constraint must be applied also after the iteration, by averaging all elements which should be identical. Doing this produces the iterative form

$$x_{i+1}=g(x_i;p,\varepsilon) \tag{8}$$

with $g=N/D$, and [for $B(3/2)$]:

$$\begin{aligned} N=&(109-122p+13p^2)+(1788-1752p-96\varepsilon+156p^2 \\ &+672p\varepsilon)x+(10560-2304p-14208\varepsilon-576p^2 \\ &+4992p\varepsilon+13824\varepsilon^2)x^2+(32768-135168\varepsilon+45056p \\ &-1024p^2-30720p\varepsilon+138240\varepsilon^2)x^3 \end{aligned}$$

and $D=768(1+8x)^2$. [A similar form holds for $B(2)$.] The fixed-point equation $x_{i+1}=x_i$ reduces to a simple cubic in x whose coefficients are low-order polynomials in p and ε, admitting simple analytical solution.

In the following we present the solution for $B(3/2)$; the results for $B(2)$ are parallel and yield identical exponents. For $\varepsilon=0$, the fixed-point equation has two solutions:

$$\begin{aligned} x_{pinned}&=1/4, \\ x_{mobile}&=[-91+140p-13p^2-3(1+p) \\ &\quad\times\sqrt{145-122p+13p^2}]/[32(16-44p+p^2)], \end{aligned} \tag{9}$$

both shown in Fig. 1. The former corresponds to $v=0$ (that is, pinned). The latter, when within a physically allowable range $(0<x<1/4)$, corresponds to a mobile phase $(0<v<1)$.

The stability of the fixed points helps us to isolate the proper behavior. Starting with a fixed-point solution (taking $\varepsilon=0$ for simplicity) $x_{FP}=g(x_{FP};p)$, expanding Eq. (8) in small δx; this gives $\delta x_{i+1}=\Gamma(p)\,\delta x_i$, where $\Gamma(p)$ $\equiv\partial g(x;p)/\partial x|_{x=x_{FP}}$. Thus $|\Gamma(p)|<1$ is the condition for stability. In Fig. 2, $\Gamma(p)$ is plotted for both fixed points. For $p<p_c$, the pinned phase is stable; solving $\Gamma(p_c)=1$ for p_c gives $p_c=(77-20\sqrt{13})/9=0.543219$. Above p_c the pinned phase is unstable. For $p>p_c$ the mobile phase is stable.

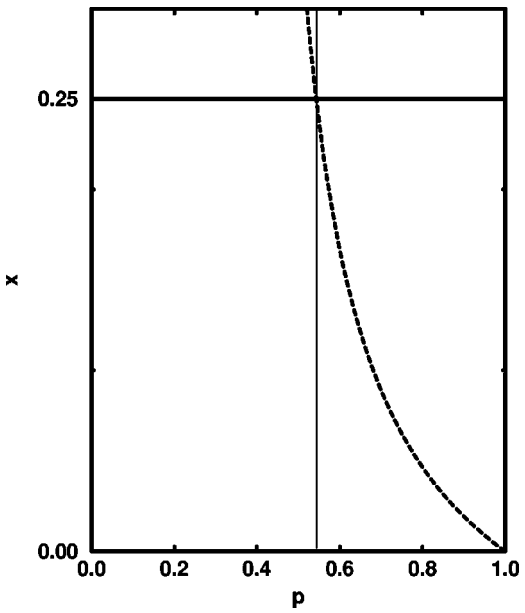

FIG. 1. Two solutions of the fixed-point equation for $B(3/2)$ with $\varepsilon=0$. The solid (horizontal) line is the pinned solution, and the dashed line is the mobile solution. The two solutions cross at $p=p_c$, which is indicated by the vertical line.

From the mobile solution for $\tilde{p}\equiv p-p_c>0$, we find easily that $v(\tilde{p})\sim\tilde{p}$, so that $\nu=1$. The relaxation time is obtained from $\tau=-1/\ln(\Gamma)$, and $\tau\sim\tilde{p}^{-1}$ near the transition, so

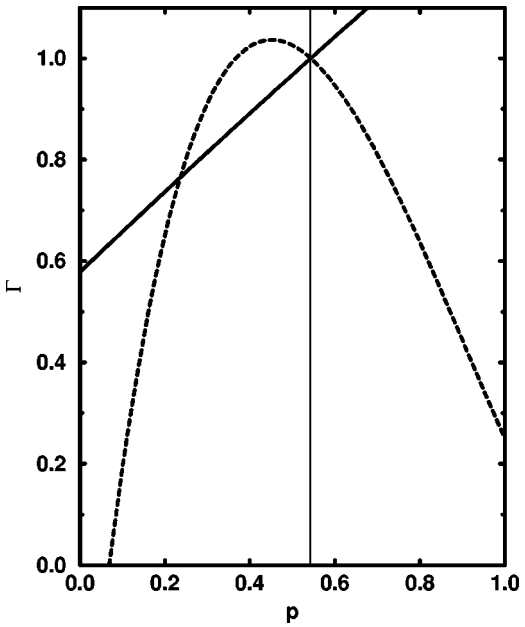

FIG. 2. Stability parameter for the two solutions (shown in Fig. 1) of the fixed-point equation for $B(3/2)$ with $\varepsilon=0$. The solid line is the pinned solution, and the dashed line is the mobile solution. The two solutions have a value of $\Gamma=1$ where they cross at $p=p_c$, which is indicated by the vertical line.

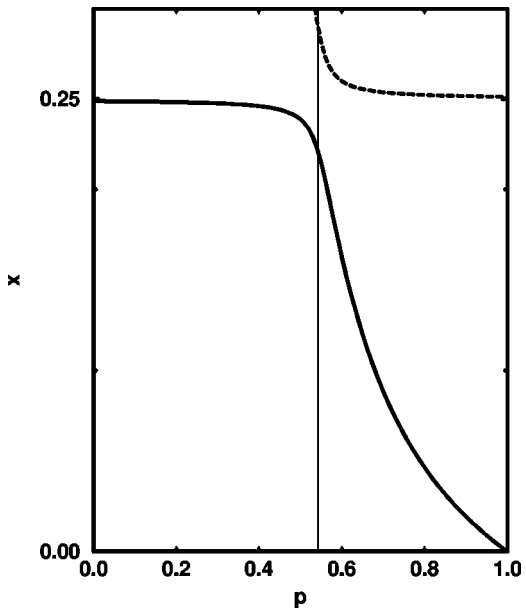

FIG. 3. Two solutions of the fixed-point equation for $B(3/2)$ with $\varepsilon>0$. The solid (horizontal) line is the physical solution, and the dashed line is unphysical. The two solutions approach in the neighborhood of $p=p_c$, which is indicated by the vertical line (compare to Fig. 1 for $\varepsilon=0$).

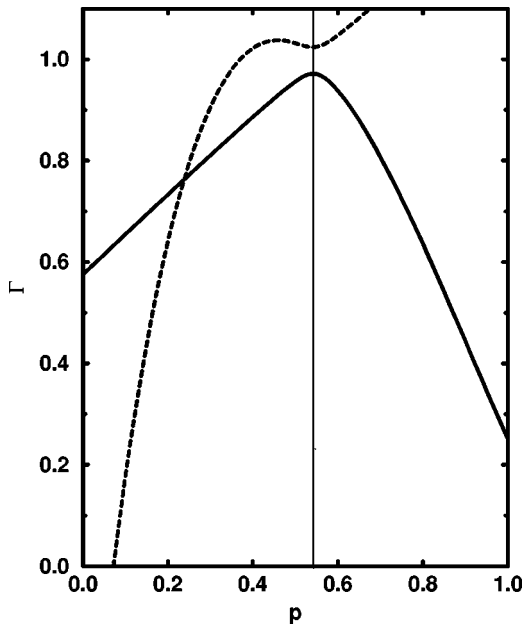

FIG. 4. Stability parameter for the two solutions (shown in Fig. 3) of the fixed-point equation for $B(3/2)$ with $\varepsilon>0$. The solid line is the physical solution, and the dashed line is the unphysical solution. The two solutions have a value of approach at $p=p_c$, which is indicated by the vertical line (compare to Fig. 2 for $\varepsilon=0$).

that $\phi=1$. These values are compared to the numerical solutions of the exact equations in Table I.

For finite ε, the fixed-point equation has only one physical solution. The physical solution and a neighboring unphysical one are plotted in Fig. 3. Comparing to the solutions for $\varepsilon=0$ (Fig. 1) shows that finite ε opens up a gap between the two solutions; the gap vanishes as $\varepsilon\to 0$. The corresponding stability parameters Γ are plotted in Fig. 4. Comparing to Fig. 2, one sees that the gap between the two solutions vanishes as $\varepsilon\to 0$.

In Fig. 5 the solution is plotted for ε varied over six decades to show the rounding of the transition. Similarly, the velocity is plotted in Fig. 6.

The scaling behavior previously noted in the numerical work CD is analytically accessible here. It is simple to analyze the fixed-point equation [Eq. (8)] for small $\tilde{x}=x-1/4$, $\tilde{p}$, and ε. From this, one finds that $v(\tilde{p},\varepsilon)=\sqrt{\varepsilon}f(\tilde{p}/\sqrt{\varepsilon})$, thus $\beta=1/2$ and $\gamma=1/2$. Similarly, $\tau(\tilde{p},\varepsilon)=\varepsilon^{-1/2}h(\tilde{p}/\sqrt{\varepsilon})$, so that $\zeta=1/2$. The scaling functions so obtained are of the form $f(\xi)=3.43+3.12\xi+1.42\xi^2$ and $h(\xi)=1/\sqrt{0.68+0.56\xi^2}$. [The above results are for $B(3/2)$, though the results for $B(2)$ differ in unimportant ways.] The analytic mean-field critical exponents thus obtained are compared to the exact numerical results in Table I.

It is clear from this simple analytical model that the transition occurs between two solutions (pinned and unpinned) and that the scaling behavior is directly related to the interaction (i.e., avoided crossing) of the two solutions.

IV. DISCUSSION

The simple deterministic, one-parameter analytical model derived here displays the pinning/depinning transition and scaling behavior of the more complicated stochastic models proposed in earlier work. The changes in the values of the critical exponents, presented in Table I, is likely due to the mean-field approximation. While we have restricted the solution presented in the previous section to a single degree of freedom, the argument can be made that this restriction is not severe. Also the means for relaxing this restriction are easily conceived.

The above solution hinges on the stability of the pinned phase; let us consider this stability and how the various ap-

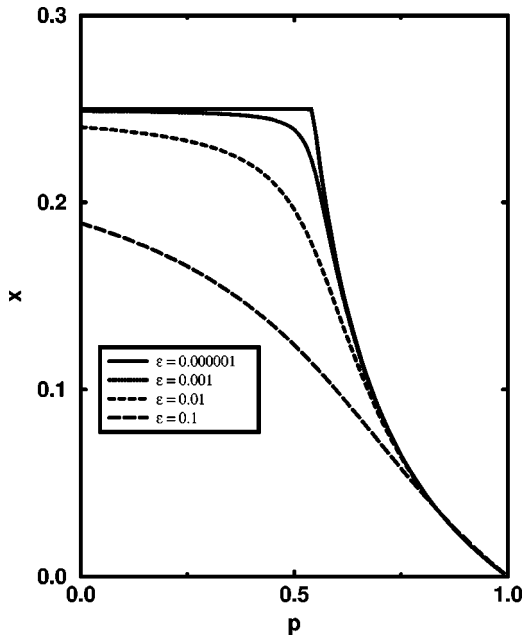

FIG. 5. Physical solution to the fixed-point equation for $B(3/2)$ over six decades of ε, illustrating the rounding of the transition at finite temperature.

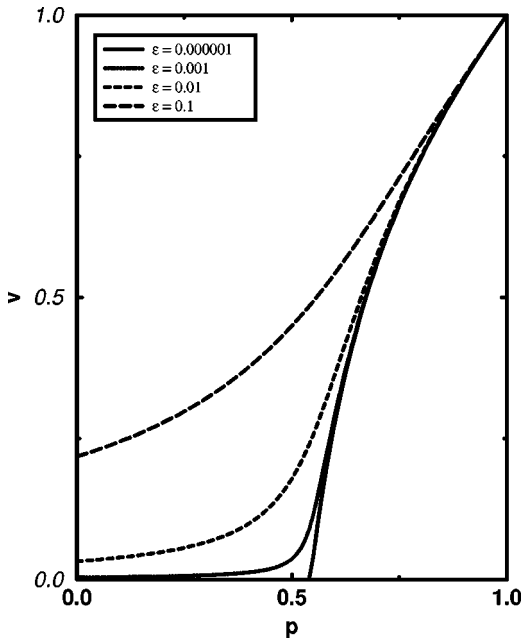

FIG. 6. The dislocation velocity for $B(3/2)$ over six decades of ε, illustrating the rounding of the transition at finite temperature.

proximations we have made may alter this stability. We will examine the case where thermal depinning vanishes and the transition is abrupt ($\varepsilon=0$). In that case, there is a well-defined pinned phase. In the full model describing a dislocation line as a series of segments, the pinned phase consists of all possible arrangements of immobile segments; for a line of length L, there are $(2M-1)^L$ such dislocations. The phase space of pinned states is contiguous and occupies a fraction $[(2M-1)/(2M+1)]^L$ of the total phase space. As M increases (as in the present study, from $M=3/2$ to $M=2$), the pinned phase occupies a larger fraction of the total phase space, and this largely explains the increase in p_c with M. For $p<p_c$, perturbations in the pinned phase are stable, in the sense that a pinned state evolves through a sequence of mobile configurations to another pinned state. Thus the trajectory through the mobile space connects two points in the immobile space.

In the mean-field approximation, the system is described by a population matrix. The pinned phase is still highly degenerate: any population matrix with vanishing mobile population is a fixed point.

Constraining the mean-field solution to the single-parameter form [Eq. (6)] collapses the space of the pinned phase to a single point (i.e., all pinned states are the same). By contrast, the mobile phase is contracted to a line extending from the pinned phase.

Given these considerations, it is somewhat surprising that the transition and scaling behaviors survive. In future work, we will study the relaxation of the constraint [Eq. (6)] to include more degrees of freedom (more dimensions for the pinned phase space). In this case, Γ becomes a matrix, and we analyze the eigenvalues of this stability matrix. Some eigenvalues will correspond to perturbations from one pinned state to another. Others will correspond to decay from a pinned state to a mobile one, and the transition occurs when one of these eigenvalues crosses 1. For these reasons, we expect this analysis to lead to a simple, but more complete understanding of the pinning/depinning transition.

V. CONCLUSIONS

In conclusion, we have found simple solutions to an approximate mean-field equation for the models presented in CD. These models mimic superdislocation motion in the $L1_2$ compounds displaying the yield strength anomaly, including cross-slip pinning and thermal annihilation of the pinning points.

It is verified that the models display a critical behavior. In particular, it is found that various quantities related to mechanical properties should scale for $p\approx p_c$.

It is also noted that for $\varepsilon\neq 0$, that the critical point at p_c is no longer present. However, remnants of the scaling behavior associated with that critical point that are present for small ε allow one to develop a scaling analysis to determine critical exponents associated with the $\varepsilon=0$ critical point.

ACKNOWLEDGMENTS

The authors acknowledge extensive discussions with Professor D. Chrzan (U.C. Berkeley). M.S.D. acknowledges support from the National Science Foundation, Division of Materials Theory.

*Present address: Computational Materials Group, Motorola, 3501 Ed Bluestein, Austin, Texas 78721.

[1] D.C. Chrzan and M.J. Mills, Phys. Rev. Lett. **69**, 2795 (1992).
[2] D.C. Chrzan and M.J. Mills, Phys. Rev. B **50**, 30 (1994).
[3] D. C. Chrzan and M. J. Mills, in *Dislocations in Solids*, edited by F. Nabarro and M. Duesbery (Elsevier, Amsterdam, 1996), Vol. 10, p. 187.
[4] D.C. Chrzan, M.J. Mills, and S.H. Goods, Mater. Sci. Eng., A **192/193**, 120 (1995).
[5] D.C. Chrzan and M.S. Daw, Phys. Rev. B **55**, 798 (1997).
[6] M.J. Mills and D.C. Chrzan, Acta Metall. Mater. **40**, 3051 (1992).